Infrared absorption, laser excitation and crystal-field analyses of the C_{4v} symmetry centre in KY_3F_{10} doped with Pr^{3+}

2000 J. Phys.: Condens. Matter 12 5297

(http://iopscience.iop.org/0953-8984/12/24/318)

J. Phys.: Condens. Matter **12** (2000) 5297–5306. Printed in the UK PII: S0953-8984(00)11923-X

Infrared absorption, laser excitation and crystal-field analyses of the C_{4v} symmetry centre in KY_3F_{10} doped with Pr^{3+}

Jon-Paul R Wells†§, Mitsuo Yamaga‡, Thomas P J Han† and Hugh G Gallagher†

† Optical Materials Research Centre, Department of Physics and Applied Physics, University of Strathclyde, Glasgow G1 1XN, Scotland, UK
‡ Department of Electronics, Faculty of Engineering, Gifu University, Gifu 501-1193, Japan

E-mail: wells@rijnh.nl

Received 17 February 2000

Abstract. We report a comprehensive spectroscopic study of KY_3F_{10} doped with trivalent praseodymium. Employing both infrared absorption and laser excited fluorescence spectroscopy, we have constructed an energy level scheme of 39 crystal-field states. A C_{4v} symmetry, conventional crystal-field analysis can well account for the measured crystal-field splittings with the exception of the $^1D_2$ levels. The inclusion of spin correlation effects improves the fit significantly; however the magnitudes of the optimized parameters are not well determined.

1. Introduction

Crystals offering isovalent substitution of a trivalent rare-earth ion with a lattice cation (such as Y^{3+}) have received much attention from spectroscopists and laser physicists alike. Of these, crystals of the $KF–YF_3$ system are a popular choice, an example of which is the complex fluoride host KY_3F_{10}. In part, the popularity of this class of materials may be attributed to the simplicity which arises when the need for charge compensation (for example, by interstitial anions) is absent. However these materials also offer a wide transparency, high optical damage thresholds and rigid thermomechanical properties [1], all extremely desirable features for there to be any possibility of an optically based application.

KY_3F_{10} is a cubic compound of the fluorite structure with space group O_h^5. The unit cell contains both $[KY_3F_8]^{2+}$ and $[KY_3F_{12}]^{2-}$ ionic groups which form cubes (similar to CaF_2) and cubo-octahedra of fluorine ions which alternate along the three orthogonal crystallographic directions [2, 3]. Trivalent rare-earth (RE^{3+}) ions substitute for the Y^{3+} ion and thus reside on a single site of C_{4v} point group symmetry.

Investigations into the KY_3F_{10} conduction processes [3] have shown that the electrical conductivity varies by more than 11 orders of magnitude as the temperature is increased between 100 and 770 K. The existence of two thermally activated processes attributable to different conduction pathways for fluorine vacancy motion in the crystal is postulated. Rare-earth doped KY_3F_{10} crystals have also received some attention. In particular, doping with $Sm^{3+/2+}$ [4], Eu^{3+} [5–7] and Er^{3+} [8] has been performed. In the case of samarium both the divalent and

§ Corresponding author and current address: Dr Jon-Paul R Wells, FELIX Free Electron Laser Facility, FOM Institute for Plasmaphysics 'Rijnhuizen', PO Box 1207, 3430 BE Nieuwegein, The Netherlands.

0953-8984/00/245297+10$30.00

trivalent species were observed, with the majority of ions in the divalent state. The suggestion was put forward that the Sm^{2+} centres observed could be charge compensated by fluorine vacancies under the assumption that the Sm^{2+} occupy the Y^{3+} sites. For Sm^{3+}, Eu^{3+} and Er^{3+} comprehensive crystal-field analyses have been performed. A particularly exhaustive study has been performed for KY_3F_{10}:Eu^{3+} which established Judd–Ofelt parameters through studies of the intra-4f transition moments. This information was then used to study the ^5D term multiplet non-radiative decay. Electron paramagnetic resonance studies of KY_3F_{10}:Ho^{3+} have shown the ground state in this material to consist of two close lying ($\Delta E = 7.4\ cm^{-1}$) single states whose eigenfunctions become mixed through the pseudo-quadrupole hyperfine field between them [9].

We report here on the infrared and optical spectroscopy of KY_3F_{10} crystals doped with 0.1 mol% of trivalent praseodymium ions. Using laser selective excitation and infrared absorption a total of 39 crystal-field energy levels (and their symmetry) have been determined. A C_{4v} symmetry crystal-field analysis accounts well for the inferred energy level scheme with the exception of the $^1D_2$ multiplet. The inclusion of terms in the Hamiltonian associated with a spin correlated crystal field are seen to well account for the level splittings.

2. Experiment

KY_3F_{10} crystals containing 0.1 mol% of PrF_3 were grown by the Bridgman–Stockbarger (temperature gradient) technique, using a custom built, two zone resistance heating furnace. Essentially stoichiometric amounts of YF_3 and KF were mixed together, taking into account the small amounts of PrF_3 to be added. The mixed charge was then placed in a graphite crucible which was itself placed into the furnace vacuum chamber. This was then evacuated to 10^{-6}–10^{-7} mbar so as to be free of oxygen. Ultimately, a slight positive pressure of purified argon gas was employed as the growth atmosphere to minimize evaporative losses. The crystals were lowered at a rate of 0.8 mm h^{-1} through the temperature gradient provided by the resistance coils of the furnace. After translating 10 cm, the crystals were cooled over a period of 24 hours. The as-grown crystals were up to 5 cm long and of excellent optical quality.

Laser excitation and fluorescence spectra were recorded using a 5 W Coherent Innova 70 argon ion laser to optically pump a Spectra-Physics 375B dye laser. Rhodamine 6G perchlorate dye was used to excite the $^1D_2$ multiplet of the Pr^{3+} ions, whilst $^3P_0$ was excited directly by the argon ion laser. The sample was cooled using a CTI-cryogenics model 22C cryogenic refrigerator and temperature variability was maintained by a Palm Beach Cryogenics temperature controller. Fluorescence was dispersed with a SPEX 500M single monochromator using a thermoelectrically cooled Hamamatsu R9249 photomultiplier to detect the light. Fluorescence lifetimes were measured using a Laser Science Inc. VSL-337 nitrogen laser pump dye laser. The transient was averaged using a Stanford Research Systems model SR430 multichannel averager. The integrated transients were least squares fitted to single exponential decays on a constant background for the fluorescence decay times. 0.25 cm^{-1} infrared absorption spectra were recorded with a BioRad FTS-40 Fourier transform infrared (FTIR) spectrometer over the 2000–8000 cm^{-1} spectral range to record transitions to the $^3H_5$, $^3H_6$, $^3F_2$, $^3F_3$ and $^3F_4$ multiplets. The crystal samples were mounted on a copper holder and cooled by thermal contact with the 10 K stage of a CTI LTS 0.1 closed cycle helium cryostat.

3. Spectroscopy of KY_3F_{10}:Pr^{3+}

The $4f^2$ configuration, appropriate for trivalent praseodymium, has 91 electronic states. Of these, 70 are observable in the absence of external Stark or magnetic fields for ions in centres

Table 1. Polarization selection rules for C_{4v} symmetry. σ indicates transitions which are both electric and magnetic dipole σ allowed.

	γ_1	γ_2	γ_3	γ_4	γ_5
γ_1	π	π_{md}			σ
γ_2	π_{md}	π			σ
γ_3			π	π_{md}	σ
γ_4			π_{md}	π	σ
γ_5	σ	σ	σ	σ	π, π_{md}

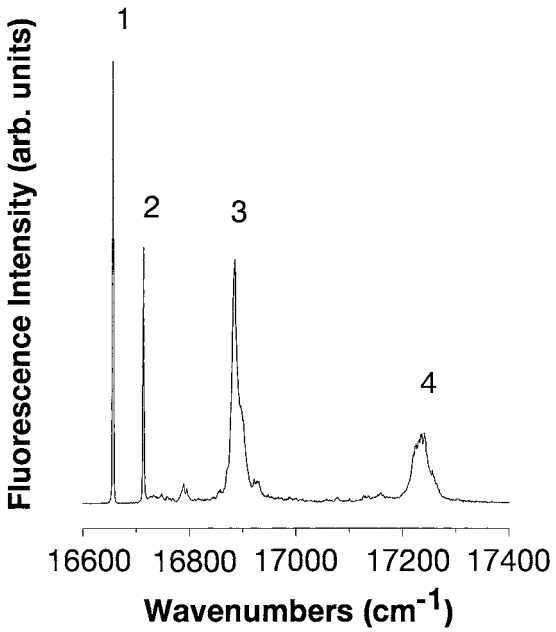

Figure 1. 10 K $^1D_2$ excitation spectrum of a KY_3F_{10} crystal doped with 0.1 mol% of Pr^{3+}.

of C_{4v} symmetry and must transform according to one of the irreducible representations ($\gamma_i, i = 1, \ldots, 5$) of the C_{4v} point group. The polarization selection rules for non-Kramers ions in sites of C_{4v} symmetry are well known, but for the purposes of the following discussion we summarize these in table 1. In general, Pr^{3+} states are labelled by the parent $^{(2S+1)}L_J$ state, an arbitrary alphabetical label (following Dieke [10]) plus a numerical subscript and their wavefunction symmetry denoted by the appropriate irreducible representation (irrep). So the ground multiplet, $^3H_4$ is Z with the ground state denoted as $^3H_4Z_1(\gamma_5)$.

3.1. Laser excitation and fluorescence

Figure 1 shows the laser excitation spectrum for the $^1D_2$ multiplet which was obtained by monitoring the fluorescence intensity of the $^1D_2 \rightarrow {}^3H_5$ transitions centred around 14 200 cm^{-1}. Any unwanted laser scatter was discriminated against using a Schott RG640 filter. The lowest $^1D_2$ states are clearly apparent as sharp transitions at 16 657 and 16 712 cm^{-1}, a situation reminiscent of the analogous spectra for Pr^{3+} in CaF_2 and SrF_2 [11]. Under C_{4v} symmetry, the $^1D_2$ multiplet is expected to be split into four crystal-field states, a γ_5 doublet and three singlets transforming as γ_1, γ_3 and γ_4 irreps. With due consideration of the

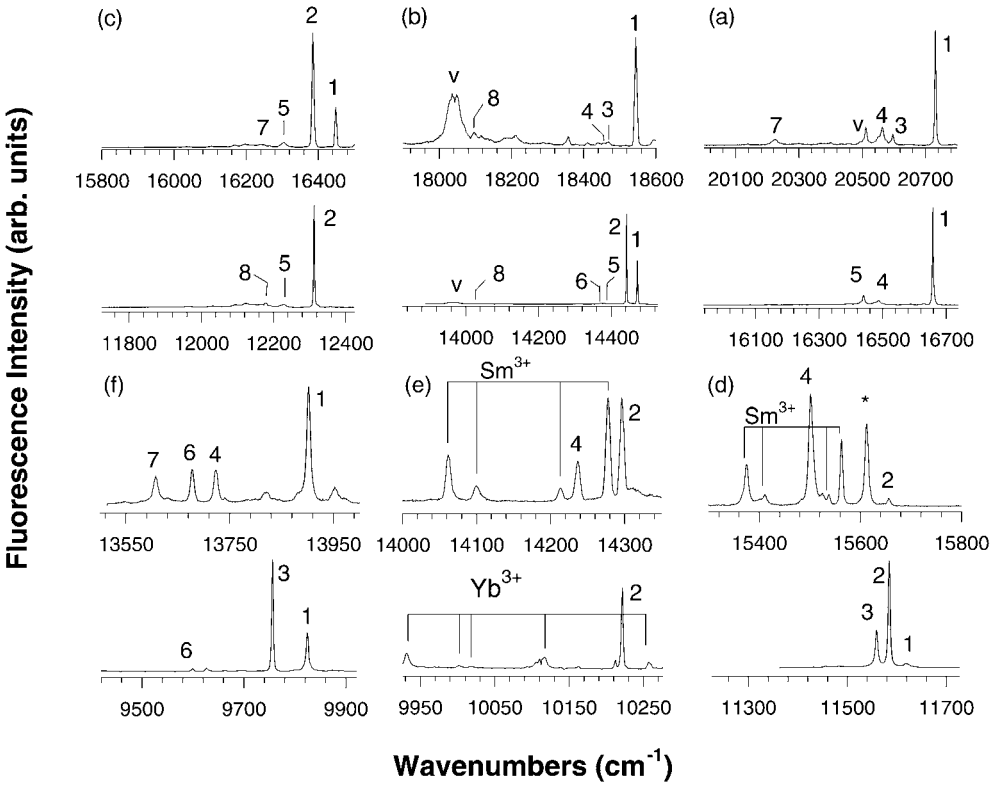

Figure 2. 10 K fluorescence spectra of the (a) $^3H_4$, (b) $^3H_5$, (c) $^3H_6$, (d) $^3F_2$, (e) $^3F_3$ and (f) $^3F_4$ multiplets. In each case the upper spectrum emanates from the $^3P_0A_1\gamma_1$ state at 20 733 cm^{-1} and the lower spectrum emanates from the $^1D_2D_1\gamma_4$ state at 16 657 cm^{-1}. The notation v is used to denote a transition terminating on a vibronic state of the lattice whilst the $*$ notation indicates an unassigned transition.

polarization selection rules listed in table 1, the observation of all four crystal-field states seems to confirm the ground state of the $^5H_3$ multiplet to be a γ_5 doublet, an assignment consistent with infrared absorption measurements presented below. A weaker broadband background extending upward in energy from 16 900 cm^{-1} can be assigned as a one phonon sideband absorption band. The sharp lines denoted by 1, 2 and 3 in figure 1 are due to the three γ_4, γ_3 and γ_1 singlet states and the broad line is due to the γ_5 doublet state as assigned from preliminary crystal-field analyses.

Figures 2(a)–(f) show fluorescence due to transitions to multiplets of the low lying ^3H and ^3F coulombic terms from the single $^3P_0$ state (upper part of each figure) and the $^1D_2$ multiplet (lower part of each figure). The ground state ($^3H_4$) is split into seven energy levels by a C_{4v} symmetry crystal-field potential, which are represented by singlet states transforming as γ_2, γ_3 or γ_4, two γ_1 symmetry orbital singlets and two doublet states which transform as γ_5 irreps. As the $^3P_0$ multiplet consists, by necessity, of a single crystal-field state transforming as a γ_1 singlet, only four electric dipole transitions to the $^3H_4$ multiplet are expected from the selection rules in table 1. Figure 2(a) shows five transitions from $^3P_0A_1\gamma_1$ to the $^3H_4$ multiplet. The line denoted by v has an energy separation (221 cm^{-1}) between the lines 1 and v, which is consistent with a host lattice longitudinal optical (LO) phonon energy. In consequence, we

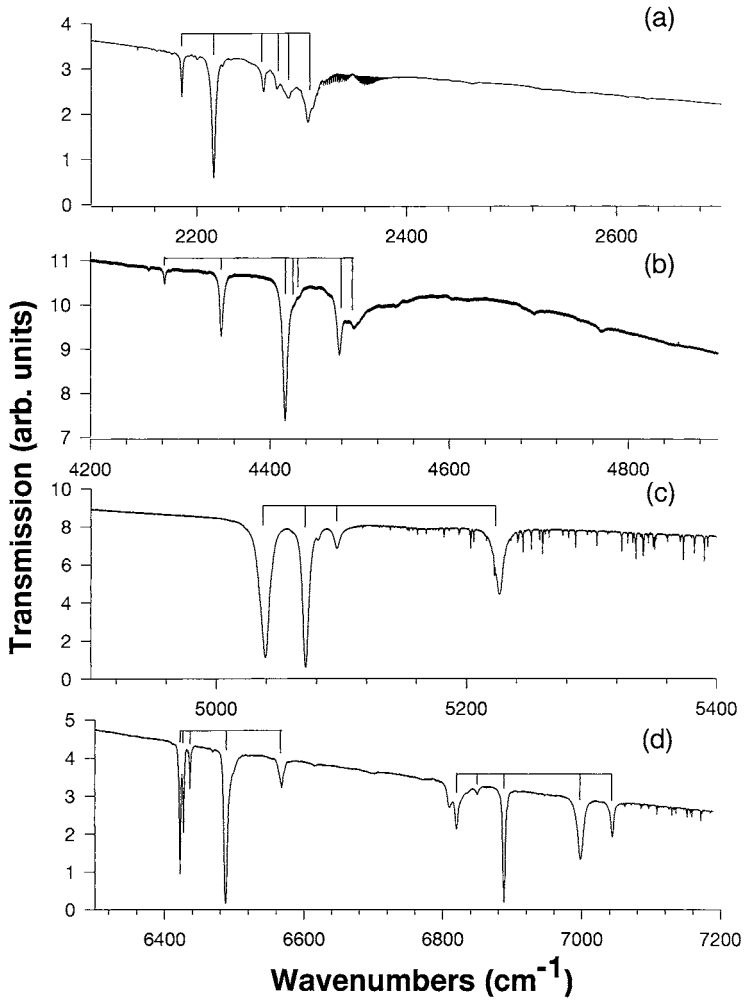

Figure 3. 10 K infrared absorption spectra of the (a) $^3H_5$, (b) $^3H_6$, (c) $^3F_2$, (d) $^3F_3$ and $^3F_4$ multiplets.

assign the $^3P_0A_1\gamma_1$ state energy as 20 733 cm^{-1}. Three fluorescence transitions (presented in the lower part of figure 2(a)) are observed from $^1D_2$ and hence the emitting state must be a singlet of other than γ_1 symmetry. Preliminary crystal-field calculations employing the KY_3F_{10}:Sm^{3+} crystal-field parameters obtained previously [4], predict the $^1D_2(D_1)$ state to have γ_4 symmetry consistent with this observation. The lines denoted by 4 in figure 2(a) have an energy separation from the ground state transition of 170 cm^{-1} and can be detected from both the $^3P_0$ and $^1D_2$ multiplets. Thus, this state must transform as a γ_5 doublet. The remaining states corresponding to the lines 3 and 7 can be assigned as γ_1 singlets with energies of 136 and 508 cm^{-1}. The line 5 in the lower part of figure 2(a) is assigned as a γ_4 singlet as it is only observed in fluorescence from $^1D_2$.

For the next excited ^3H_J ($J = 5, 6$) and ^3F_J ($J = 2, 3, 4$) multiplets, the same assignment procedure is carried out. Transitions to terminating states which are observed from both $^1D_2$ and $^3P_0$, for example, the lines 1, 5 and 8 in figure 2(b), can be assigned as doublets of γ_5

Table 2. Calculated and 10 K experimental crystal-field energy levels (as measured in air ($cm^{-1} \pm 1$) of the $^3H_4$, $^3H_5$, $^3H_6$, $^3F_2$, $^3F_3$ and $^3F_4$, $^1D_2$ and $^3P_0$ multiplets of the C_{4v} centre in KY_3F_{10}† indicates levels assigned from infrared absorption. The error on the levels inferred from LSE is ± 1 cm^{-1} whilst those measured directly by infrared absorption have an estimated uncertainty of 0.10 cm^{-1}. The SECF and SCCF notation refers to a single electron crystal-field analysis and a spin correlated crystal-field analysis respectively[a], indicates that the fit excluded the energy levels of the $^1D_2$ multiplet and the calculated levels for that fit are bracketed.

			Calculated energy levels		
Multiplet	State and symmetry	Expt	SECF[a]	SECF	SCCF
	$Z_1\gamma_5$	0	10	17	5
	$Z_2\gamma_3$	—	107	105	113
	$Z_3\gamma_1$	136	133	121	133
$^3H_4$	$Z_4\gamma_5$	170	191	169	193
	$Z_5\gamma_4$	214	200	202	204
	$Z_6\gamma_2$	—	513	539	517
	$Z_7\gamma_1$	508	520	540	517
	$Y_1\gamma_5$	2 186	2 186	2 188	2 186
	$Y_2\gamma_4$	2 216	2 215	2 222	2 218
	$Y_3\gamma_2$	—	2 214	2 223	2 214
$^3H_5$	$Y_4\gamma_1$	2 263	2 262	2 280	2 261
	$Y_5\gamma_5$	2 277	2 257	2 247	2 258
	$Y_6\gamma_3$	2 287	2 295	2 288	2 299
	$Y_7\gamma_2$	2 306.6†	2 308	2 294	2 309
	$Y_8\gamma_5$	2 636	2 620	2 648	2 622
	$X_1\gamma_1$	4 285	4 298	4 294	4 293
	$X_2\gamma_5$	4 347	4 352	4 355	4 347
	$X_3\gamma_2$	—	4 376	4 392	4 374
	$X_4\gamma_3$	4 417.6†	4 411	4 409	4 411
$^3H_6$	$X_5\gamma_5$	4 429	4 430	4 428	4 427
	$X_6\gamma_1$	4 433.4†	4 431	4 411	4 428
	$X_7\gamma_5$	4 478	4 490	4 488	4 490
	$X_8\gamma_4$	4 495	4 498	4 489	4 497
	$X_9\gamma_3$	—	4 968	5 009	4 974
	$X_{10}\gamma_4$	—	4 969	5 011	4 975
	$W_1\gamma_3$	5 042	5 043	5 039	5 033
$^3F_2$	$W_2\gamma_4$	5 075	5 065	5 050	5 058
	$W_3\gamma_5$	5 100	5 112	5 112	5 106
	$W_4\gamma_1$	5 230	5 222	5 227	5 218
	$V_1\gamma_3$	6 430.3†	6 444	6 445	6 449
	$V_2\gamma_5$	6 435	6 404	6 403	6 408
$^3F_3$	$V_3\gamma_4$	6 444.6†	6 457	6 472	6 462
	$V_4\gamma_5$	6 497	6 487	6 499	6 491
	$V_5\gamma_2$	6 576.6†	6 574	6 596	6 580
	$U_1\gamma_5$	6 831	6 835	6 836	6 821
	$U_2\gamma_3$	6 859.4†	6 845	6 852	6 856
	$U_3\gamma_4$	6 901	6 904	6 889	6 900
$^3F_4$	$U_4\gamma_1$	7 006	6 983	6 977	7 003
	$U_5\gamma_2$	—	6 988	6 979	7 004
	$U_6\gamma_5$	7 056	7 064	7 068	7 061
	$U_7\gamma_1$	7 126	7 146	7 156	7 134

Table 2. (Continued)

			Calculated energy levels		
Multiplet	State and symmetry	Expt	SECF[a]	SECF	SCCF
	$D_1\gamma_4$	16 657	(17 179)	16 677	16 658
$^1D_2$	$D_2\gamma_3$	16 712	(17 327)	16 783	16 712
	$D_3\gamma_1$	16 886	(17 336)	16 851	16 890
	$D_4\gamma_5$	17 236	(17 665)	17 181	17 232
$^3P_0$	$A_1\gamma_1$	20 733	20 738	20 730	20 739

symmetry. The remaining transitions must have the same symmetry as the emitting state under the assumption of electric dipole transitions only as is apparent from the polarization selection given in table 1. The exception to this is the $^1D_2 \rightarrow {}^3F_2$ and $^3F_3$ transition for which the magnetic dipole selection rule ($\Delta J = 0, \pm 1$) is satisfied. In these cases, fluorescence from $^1D_2D_1\gamma_4$ to states transforming as $C_{4v}\gamma_3$ irreps could be expected to be observed through a magnetic dipole transition moment. Indeed, this is the case with a transition to the $^3F_2W_1\gamma_3$ state at 5042 cm^{-1} shown in figure 2(d). Interestingly, a transition is observed from the $^3P_0A_1\gamma_1$ state which has a transition frequency of 15 658 cm^{-1}, a value consistent with assignment of the terminating state as $^3F_2W_2\gamma_4$ at 5075 cm^{-1}. However such a $\gamma_1 \rightarrow \gamma_4$ transition is forbidden under both magnetic and electric dipole selection rules for strict C_{4v} symmetry. It is necessary to consider the possibility of impurity ion transitions. As the excitation of the $^3P_0$ multiplet is non-resonant, the observed fluorescence is non-selective against unintentional impurities. Fluorescence to the $^3F_2$ and $^3F_3$ multiplets (shown in figures 2(d) and (e)) shows fluorescence transitions of Sm^{3+} ions as well as those of Yb^{3+}. Unintentional impurities such as these can be traced to either the YF_3 or PrF_3 start materials used in the growth of the crystal. Given that the 15 658 cm^{-1} transition cannot be accounted for terms of these known impurities and in light of the extremely good agreement of the energy matches, the transition is assigned as terminating on the $^3F_2W_2\gamma_4$ state.

Measurements of the $^3P_0$ and $^1D_2$ lifetimes have been made at both 10 K and room temperature using a VSL-337 nitrogen laser pumped organic dye laser. In all cases, a three parameter single exponential fit has been entirely adequate to account for the observed transients, the free parameters of which were determined using a least squares regression technique. The fitted values of the lifetimes are determined to be for $^1D_2$, $\tau(10\ \mathrm{K}) = 339 \pm 15\ \mu s$ and $\tau(300\ \mathrm{K}) = 224 \pm 10\ \mu s$. For the $^3P_0$ multiplet we obtain $\tau(10\ \mathrm{K}) = 43 \pm 2\ \mu s$ and $\tau(300\ \mathrm{K}) = 53 \pm 3\ \mu s$.

3.2. Infrared absorption

The 10 K infrared absorption spectra of the $^3H_5$, $^3H_6$, $^3F_2$, $^3F_3$ and $^3F_4$ multiplets is shown in figure 3 for a 3 mm slice of KY_3F_{10}:1%Pr^{3+}. As the ground state is an orbital doublet γ_5 for this $Pr^{3+}C_{4v}$ symmetry centre, in principle transitions to all 34 crystal-field levels of these five multiplets are allowed. At 10 K, one expects that only transitions from the ground state will be observed as the first excited state is predicted to be close to 100 cm^{-1} above the ground state in the crystal-field analyses listed immediately below and is therefore unpopulated at these temperatures. Specific transitions have been assigned by comparison with laser excited fluorescence from the $^1D_2$ and $^3P_0$ multiplets discussed above. Transitions to many Pr^{3+} states not observed via LSE due to state symmetry restrictions can also be determined and infrared absorption has positively identified the $^3H_5Y_6\gamma_3$, $^3H_5Y_8\gamma_5$, $^3H_6X_4\gamma_3$, $^3H_6X_6\gamma_1$, $^3F_3V_1\gamma_3$,

$^3F_3V_3\gamma_4$, $^3F_3V_5\gamma_2$ and $^3F_4U_2\gamma_3$ states and the measured energies of these levels are listed in table 2.

4. Single electron and spin-correlated crystal-field analyses

The crystal-field calculations presented here have been performed using the crystal-field fitting routines of Dr Mike Reid of the Department of Physics and Astronomy, University of Canterbury, NZ. The free-ion Hamiltonian has been parametrized as

$$H_{f.i.} = \sum_{k=2,4,6} F^k f_k + \sum_i \zeta l_i s_i + \alpha L(L+1) + \beta G(G_2) + \gamma G(R_7) + \sum_{h=0,2,4} m_h M^h + \sum_{f=2,4,6} p_f P^f \quad (1)$$

where the first two interactions represent the inter-electronic coulombic repulsion and spin–orbit interactions. The remaining terms represent the interaction between configurations (characterized by the parameters α, β and γ) and the spin–spin and spin–other-orbit interactions, represented by the parameters M^h with the two body electrostatically correlated magnetic interactions represented with parameters, P^f. The coulombic repulsion and spin–orbit terms represent by far the largest perturbations to the degenerate $4f^2$ configuration with the residual terms yielding smaller corrections which are nonetheless necessary to properly account for the energy level structure of Pr^{3+}. In this analysis, we treat only the Slater parameters F^k and the spin–orbit parameter ζ as freely variable parameters, the remainder fixed at those values given by Carnall *et al* [12]. The Pr^{3+} ion is characterized by significant mixing of the Russell–Saunders free-ion terms through off diagonal matrix elements of the spin–orbit interaction. This is the situation commonly referred to as intermediate coupling. The largest contributions [13] are 3% of $^1G_4$ in $^3H_4$, 2% of $^1D_2$ character in $^3F_2$ and 32% of $^1G_4$ in $^3F_4$. The remaining terms were essentially 100% pure LS coupled states.

The energy levels of Pr^{3+} in KY_3F_{10} have been fitted to a Hamiltonian, appropriate for C_{4v} symmetry, using the entire 91 electronic energy levels of the $4f^2$ configuration as basis states. The Hamiltonian has the form:

$$H_{C_{4v}} = B_0^2 C_0^{(2)} + B_0^4 C_0^{(4)} + B_0^6 C_0^{(6)} + B_4^4 (C_4^{(4)} + C_{-4}^{(4)}) + B_4^6 (C_4^{(6)} + C_{-4}^{(6)})$$

where all symbols are as defined in Wybourne [14]. Table 2 presents fits to the experimental data both including and excluding the energy levels of the $^1D_2$ multiplet. As can be seen, there is an excellent fit to the data if the $^1D_2$ multiplet energy levels are omitted but upon the inclusion of these states the fit degrades significantly and the standard deviation of the fit is effectively doubled. One possibility to account for this is to extend the phenomenological crystal-field model we use to include the effects of spin polarization of the individual 4f electrons. We do this in terms of the spin correlated crystal-field (SCCF) [15, 16], the physical basis of which is derived from the fact that spin parallel electrons occupy more compact orbitals (due to attractive exchange forces) than spin anti-parallel electrons. Therefore spin anti-parallel electrons are likely to be subject to stronger interactions with their surrounding environment. A crystal-field Hamiltonian is employed which we define as:

$$H_{SCCF} = \sum_{k,q,i} \left(B_q^k + b_q^k \boldsymbol{s}_i \cdot \boldsymbol{S} \right) C_q^{(k)}(i)$$

where $\boldsymbol{s}_i$ and $\boldsymbol{S}$ denote the one electron and total spin operators respectively and b_q^k is a spin correlated crystal-field parameter. The B_q^k are the standard one electron crystal-field parameters and the $C_q^{(k)}$ are the Racah spherical tensors defined as before [14]. As such, for each single

Table 3. Optimized free-ion and crystal-field parameters for KY_3F_{10}:Pr^{3+}. All values are in cm^{-1} with the exception of n, the number of experimental data points and the c_q^k. a indicates that the energy levels of the $^1D_2$ multiplet have not been included in the fit. The c_q^k values in round brackets are poorly determined with respect to their sign and magnitude.

Parameters	SECF[a]	SECF	SCCF
F^2	70 301	68 774	68 803
F^4	50 925	50 755	50 857
F^6	35 955	33 117	33 184
α	[22.9]	[22.9]	[22.9]
β	[−674]	[−674]	[−674]
γ	[1520]	[1520]	[1520]
M^{tot}	[1.76]	[1.76]	[1.76]
P^{tot}	[275]	[275]	[275]
ζ	745	746	745
B_0^2	−644	−739	−1038
B_0^4	−1543	−1535	−1690
B_4^4	343	251	123
B_0^6	891	1020	732
B_4^6	−30	54	−165
b_0^2	—	—	397
b_0^4	—	—	118
b_4^4	—	—	223
b_0^6	—	—	200
b_4^6	—	—	129
c_0^2	—	—	−0.38
c_0^4	—	—	−0.07
c_4^4	—	—	(1.81)
c_0^6	—	—	0.27
c_4^6	—	—	(−0.78)
n	35	39	39
σ	14	26	13

electron crystal-field parameter we have a SCCF parameter and the parameter set is merely doubled. Table 2 shows the fit obtained to this extended Hamiltonian. As can be seen a substantial improvement is achieved with the $^1D_2$ splitting well accounted for. The standard deviation of the fit is seen to drop from 26 to 13 cm^{-1}. Table 3 shows the fitted parameters. The values of the $c_q^k = b_q^k/B_q^k$ ratios seem physically reasonable (with the exception of c_4^4 and c_6^6 which are poorly determined) although large, apparently indicating the significance of spin correlation effects in KY_3F_{10}. If the c_q^k are to correspond to an orbital contraction their sign should be negative and it is noted that both c_4^4 and c_0^6 are positive. This has been explained in [16] in terms of a positive covalent contribution. However it is also noted that several of the single electron parameters have changed considerably, perhaps most notably the value of B_0^2. It is unlikely that changes in the single electron parameters of this magnitude are reasonable and the SCCF fit, although tempting to accept, should be treated with caution.

5. Conclusions

We have reported the first comprehensive spectroscopic investigation of KY_3F_{10} doped with trivalent praseodymium. We find the presence of a single Pr^{3+} centre with C_{4v} symmetry in accordance with its substitution for trivalent yttrium. From a combination of laser excitation

and infrared absorption we have been able to construct an energy level scheme for 36 crystal-field states of the low lying multiplets. Single electron crystal-field analyses well account for the observed splitting with the exception of the $^1D_2$ multiplet. A partial attempt to account for electron correlation effects has been attempted via the inclusion of terms in the crystal-field Hamiltonian corresponding to a spin correlated crystal field. Whilst excellent agreement is obtained between the measured and calculated crystal-field states, the exact magnitudes of the optimized crystal-field parameters are poorly determined. This situation may be remedied with a more extensive experimental data set.

Acknowledgments

This work was funded in the United Kingdom by the Engineering and Physical Sciences Research Council (EPSRC) under research contract GR/K/8802 and the British council via a joint research award. Technical assistance has been provided by D Clark and R G Dawson. The authors would like to thank Dr M F Reid of the Department of Physics and Astronomy, University of Canterbury, NZ for allowing the use of his crystal field fitting programs and useful discussions. In addition, we wish to thank Dr Glynn D Jones (Department of Physics and Astronomy, University of Canterbury, NZ) for allowing the use of a Digilab FTS-40 Bio-Rad FTIR to measure the infrared absorption spectra.

References

[1] Dubinskii M A, Khaidukov N M, Garipov I G, Dem'yanets L N, Naumov A K, Semashko V V and Malyusov V A 1990 *J. Mod. Opt.* **37** 1355
[2] Mortier M, Gesland J Y, Rousseau M, Pimenta M A, Laderia L O, Machado da Silva J C and Barbosa G A 1991 *J. Raman Spectrosc.* **22** 393
[3] Ayala A P, Olivera M A S, Gesland J Y and Moreira R L 1998 *J. Phys.: Condens. Matter* **10** 5161
[4] Wells J-P R, Sugiyama A, Han T P J and Gallagher H G 1999 *J. Lumin.* **85** 91
[5] Porcher P and Caro P 1976 *J. Chem. Phys.* **65** 89
[6] Porcher P and Caro P 1978 *J. Chem. Phys.* **68** 4176
[7] Porcher P and Caro P 1978 *J. Chem. Phys.* **68** 4183
[8] Heyde K, Binnemans K and Gorller-Walrand G 1998 *J. Chem. Soc. Faraday Trans.* **94** 1671
[9] Malkin B Z and Tarasov V F and Shakurov G S 1995 *JETP Lett.* **62** 811
[10] Dieke G H 1968 *Spectra and Energy Levels of Rare-Earth Ions in Crystals* (New York: Interscience)
[11] Reeves R J, Jones G D and Syme R W G 1992 *Phys. Rev.* B **46** 5939
[12] Carnall W T, Goodman G L, Rajnak K and Rana R S 1989 *J. Chem. Phys.* **90** 3443
[13] Wells J-P R, Jones G D and Reeves R J 1999 *Phys. Rev.* B **60** 851
[14] Wybourne B G 1965 *Spectroscopic Properties of Rare Earths* (New York: Interscience)
[15] Judd B R 1977 *Phys. Rev. Lett.* **39** 242
[16] Newman D J, Siu G G and Fung W Y P 1982 *J. Phys. C: Solid State Phys.* **15** 3113